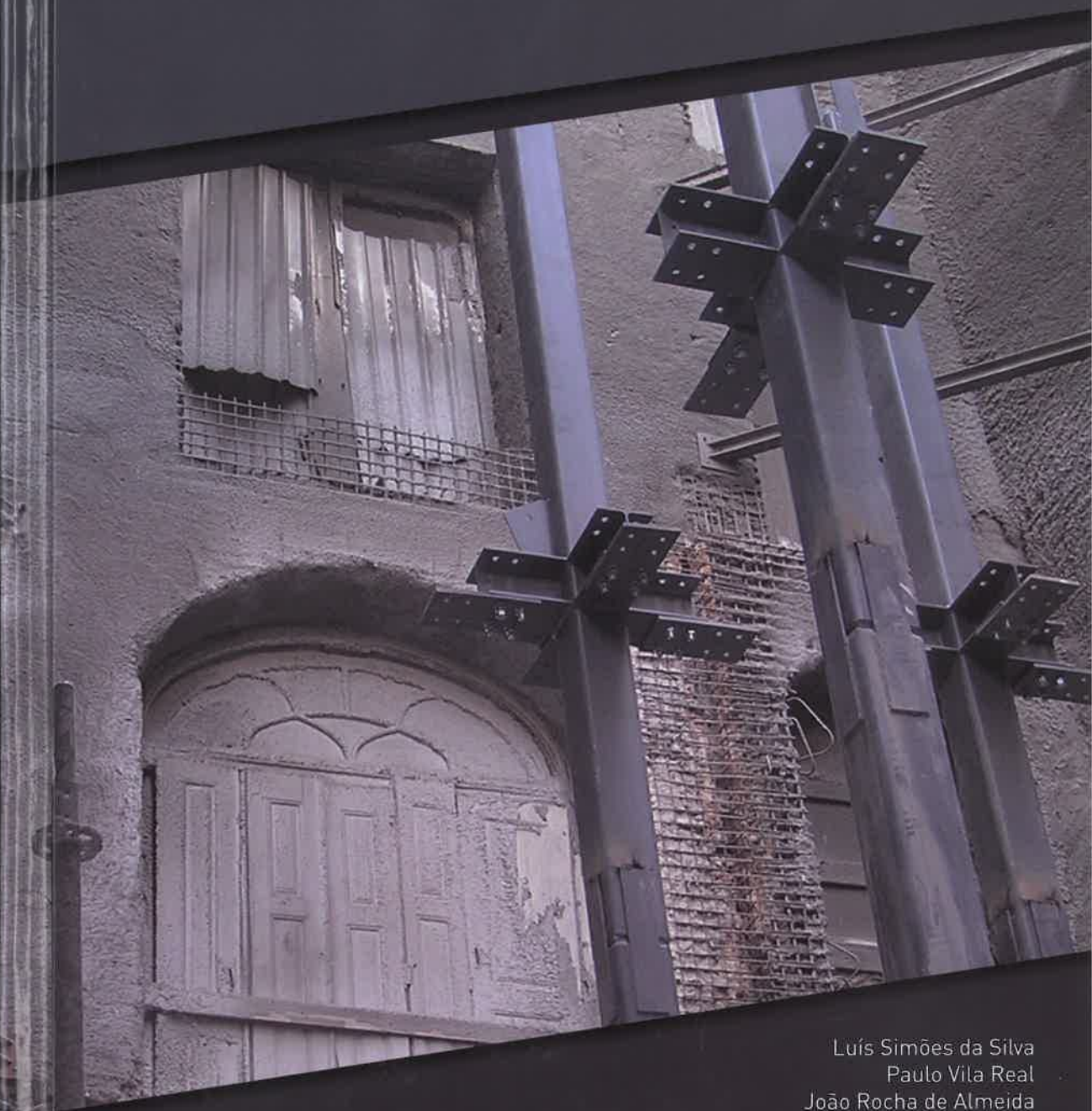


X CONGRESSO DE CONSTRUÇÃO METÁLICA E MISTA

TEMA ESPECIAL: REABILITAÇÃO DO AMBIENTE CONSTRUÍDO



Luís Simões da Silva
Paulo Vila Real
João Rocha de Almeida
Rodrigo Gonçalves



cmm

ASSOCIAÇÃO
PORTUGUESA
DE CONSTRUÇÃO
METÁLICA E MADEIRA

Secretariado da CMM

Business Center Leonardo Da Vinci, It.3 iParque,
3040-540 Antanhol, Coimbra, Portugal

cmm@cmm.pt

www.cmm.pt

com o apoio de:



UNIVERSIDADE
NOVA
DE LISBOA



FACULDADE DE
CIÊNCIAS E TECNOLOGIA
UNIVERSIDADE NOVA DE LISBOA



AXIAL BUCKLING LOAD OF PARTIALLY ENCASED COLUMNS UNDER FIRE – NEW FORMULAE

Paulo Piloto ^{a,*}, Luís Mesquita ^a, A. B Ramos-Gavilán ^b and David Almeida ^a

^{a,b} *Polytechnic Institute of Bragança, Portugal*

^c *University of Salamanca, Spain*

Abstract. Fire resistance of partially encased columns (HEB and IPE) depends on the temperature evolution during fire exposure. This paper aims to assess the effect of the balanced summation model into the design of the axial buckling load of partially encased columns under fire, according to EN 1994-1-2. New formulae will be proposed to evaluate the fire resistance, based on new simple formulas to determine the flange temperature, the residual height and temperature of the web, the residual cross section and temperature of concrete, the reduced stiffness and strength of reinforcement. ANSYS was used to validate new and safe formulae, based on the analysis of the cross section totally engulfed in fire.

1. Introduction

Partially encased columns are usually made of hot rolled steel profiles, reinforced with concrete between the flanges. The composite section is responsible for increasing the torsional and bending stiffness when compared to the same section of the steel profile. In addition to these advantages, the reinforced concrete is responsible for increasing the fire resistance. The fire resistance of partially encased columns depends on the temperature effect in each component. According to Eurocode 4, Part 1.2 [1], the fire resistance can be evaluated by balanced summation method of four components (the flanges of steel profile, the web of steel profile, concrete and reinforcement) when submitted to standard fire and for different fire resistance classes (R30, R60, R90 and R120). This paper aims to assess the parameters of Annex G: average temperature of the flange, part of the web to be neglected, residual area and average temperature of the concrete and the reduction of reinforcement mechanical properties and their influence into the axial buckling load. Two types of cross section were selected to study the effect of fire, corresponding to a set of cross section geometries: IPE ranging from 200 to 500 and HEB ranging from 160 to 500. The axial design buckling load was also calculated for two different column lengths (3 and 5 m) and three different boundary conditions originating three different buckling lengths in fire conditions (pinned at both extremities, clamped in both extremities and pinned – clamped boundary conditions). Fig. 1 represents the generic partially

encased column, identifies the four components, shows the finite element model, presents the deformed shape mode under axial load and the buckling length in fire conditions.

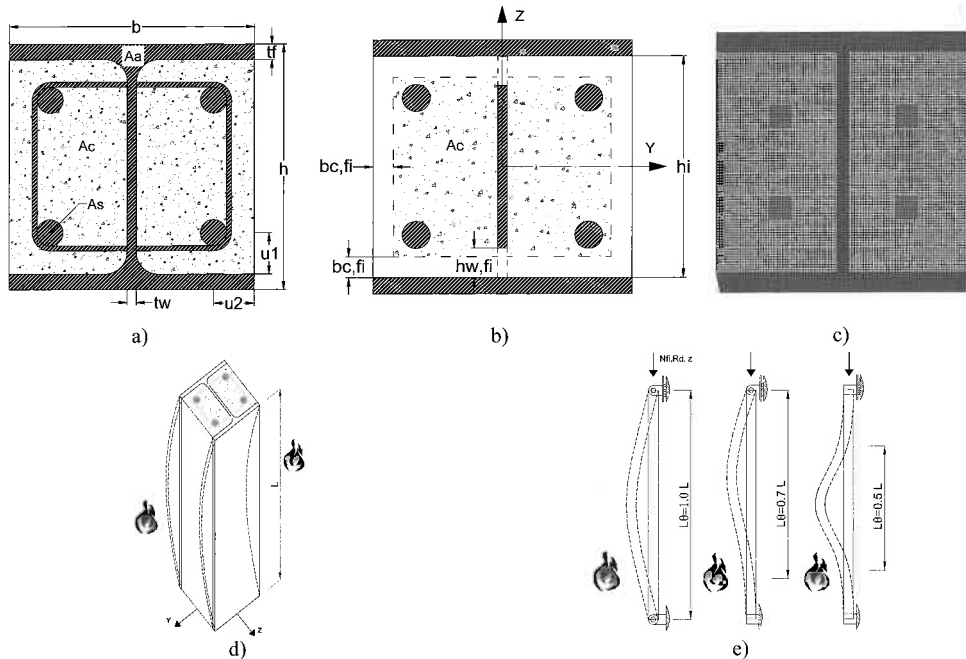


Fig. 1: Partially encased column: a) Cross section model; b) parameters; c) FE approximation; d) buckling deformed shape mode; e) Buckling length in fire

The nonlinear solution method (ANSYS) was used to evaluate the temperature field. The finite element method requires the solution of Eq. 1 in the cross section domain and Eq. 2 in the boundary. In these equations: T represents the temperature of each material; ρ defines the specific mass; $C_{p(T)}$ defines the specific heat; $\lambda_{(T)}$ defines the thermal conductivity; α_c specifies the convection coefficient; T_g represents the gas temperature of the fire compartment; Φ specifies the view factor; ϵ_m represents the emissivity of each material; ϵ_f specifies the emissivity of the fire; σ represents the Stefan-Boltzmann constant. The standard fire curve ISO 834 [2] is assumed around the cross section (4 exposed sides).

$$\nabla \cdot (\lambda_{(T)} \cdot \nabla T) = \rho_{(T)} \cdot C_{p(T)} \cdot \partial T / \partial t \quad (\Omega) \quad (1)$$

$$(\lambda_{(T)} \cdot \nabla T) \cdot \vec{n} = \alpha_c (T_g - T) + \Phi \cdot \epsilon_m \cdot \epsilon_f \cdot \sigma \cdot (T_g^4 - T^4) \quad (\partial\Omega) \quad (2)$$

The analysis of the thermal results allows to apply specific criteria to define the main parameters to calculate the plastic resistance to axial compression $N_{fi,pl,Rd}$ and the effective flexural stiffness $(EI)_{fi,eff,z}$ of the cross section under fire condition, according to Eqs. 3-4.

$$N_{fi,pl,Rd} = N_{fi,pl,Rd,f} + N_{fi,pl,Rd,w} + N_{fi,pl,Rd,c} + N_{fi,pl,Rd,s} \quad (3)$$

$$(EI)_{fi,eff,z} = \varphi_{f,\theta} (EI)_{fi,f,z} + \varphi_{w,\theta} (EI)_{fi,w,z} + \varphi_{c,\theta} (EI)_{fi,c,z} + \varphi_{s,\theta} (EI)_{fi,s,z} \quad (4)$$

The weighting parameters $\varphi_{i,\theta}$ depend on the effect of thermal stresses. The values are given in Table 1. The contribution of each component depends on the temperature effect. This

simple calculation method allows to determine the design axial load of partially encased columns under fire condition.

Table 1: Reduction coefficients for bending stiffness around weak axis

Standard Fire resistance	$\varphi_{f,\theta}$	$\varphi_{w,\theta}$	$\varphi_{c,\theta}$	$\varphi_{s,\theta}$
R30	1,0	1,0	0,8	1,0
R60	0,9	1,0	0,8	0,9
R90	0,8	1,0	0,8	0,8
R120	1,0	1,0	0,8	1,0

The Euler buckling or elastic critical load follows Eq. 5, where L_θ represents the buckling length of the column under fire conditions. The non-dimensional slenderness ratio may be calculated using Eq. 6, when the safety partial factors are equal to 1.0.

$$N_{fi,cr,z} = \pi^2 / L_\theta^2 \times (EI)_{fi,eff,z} \tag{5}$$

$$\bar{\lambda}_\theta = \sqrt{N_{fi,pl,Rd} / N_{fi,cr,z}} \tag{6}$$

The design axial buckling load under fire may be calculated according to Eq. 7, using the buckling curve “c” of EN1993-1-1 [3] and the reduction coefficient χ_z [1].

$$N_{fi,Rd,z} = \chi_z \times N_{fi,pl,Rd} \tag{7}$$

2. Partially encased columns

The cross sections were designed according to the tabulated method applied to column design under fire conditions [1], considering the minimum reinforcement ratio $A_s / (A_s + A_c)$, the minimum concrete cover dimensions u and the minimum cross section dimensions b, h . Table 2 presents the main dimensions, in particular the number of rebars, the diameter of each rebar Φ and the concrete cover dimensions in both principal directions, u_1, u_2 . Two different length (3 and 5 m) and three different buckling length (0.5L, 0.7L and 1.0L) were considered for columns.

Table 2: Section properties

Profile	Rebars	h_i mm	Φ mm	A_s mm ²	A_c mm ²	u_1 mm	u_2 mm	u mm	$A_s / A_s + A_c$	t_w / t_f	A_m / V m ⁻¹
HEB160	4	134.0	12	452	19916	40	40	40	2,22	0,62	25.00
HEB180	4	152.0	12	452	25616	40	40	40	1,74	0,61	22.22
HEB200	4	170.0	20	1257	31213	50	50	50	3,87	0,60	20.00
HEB220	4	188.0	25	1963	37611	50	50	50	4,96	0,59	18.18
HEB240	4	206.0	25	1963	45417	50	50	50	4,14	0,59	16.67
HEB260	4	225.0	32	3217	53033	50	50	50	5,72	0,57	15.38
HEB280	4	244.0	32	3217	62541	50	50	50	4,89	0,58	14.29
HEB300	4	262.0	32	3217	72501	50	50	50	4,25	0,58	13.33
HEB320	4	279.0	32	3217	77275	50	50	50	4,00	0,56	12.92
HEB340	4	297.0	40	5027	80509	50	50	50	5,88	0,56	12.55
HEB360	4	315.0	40	5027	85536	50	50	50	5,55	0,56	12.22
HEB400	4	352.0	40	5027	95821	70	50	59	4,98	0,56	11.67
HEB450	4	398.0	40	5027	108801	70	50	59	4,42	0,54	11.11
HEB500	4	444.0	40	5027	121735	70	50	59	3,97	0,52	10.67
IPE200	4	183.0	12	452	16823	50	40	45	2,62	0,66	30.00
IPE220	4	201.6	20	1257	19730	50	40	45	5,99	0,64	27.27
IPE240	4	220.4	20	1257	23825	50	40	45	5,01	0,63	25.00
IPE270	4	249.6	25	1963	30085	50	40	45	6,13	0,65	22.22
IPE300	4	278.6	25	1963	37848	50	40	45	4,93	0,66	20.00
IPE330	4	307.0	25	1963	44854	50	40	45	4,19	0,65	18.56
IPE360	4	334.6	32	3217	50988	50	40	45	5,93	0,63	17.32
IPE400	4	373.0	32	3217	60715	70	40	53	5,03	0,64	16.11
IPE450	4	420.8	32	3217	72779	70	40	53	4,23	0,64	14.97
IPE500	4	468.0	40	5027	83800	70	50	59	5,66	0,64	14.00

3. Advanced calculation method

The temperature field was determined by the finite element method, using ANSYS. The plane element PLANE55 was selected to perform a nonlinear transient thermal analysis. This element uses linear interpolation functions with 4 integration points to determine the conductivity matrix, see Fig. 2. The model used 4, 6 and 8 elements in the web thickness, flange thickness and reinforcement (both directions), respectively. Perfect contact between materials or components was considered. Standard fire boundary conditions were applied in the exposed surface, according to EN1991-1-2 [4].

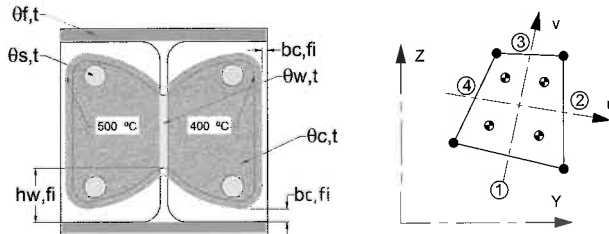


Fig. 2: Criteria to determine each component and Finite element "PLANE55"

Fig. 3 shows the temperature field corresponding to different fire resistance rating classes.

Material properties were defined according to the corresponding Eurocode for steel EN1993-1-2 [5] and concrete EN1992-1-2 [6], whereas with 3% water content by weight and a thermal conductivity corresponding to the upper limit.

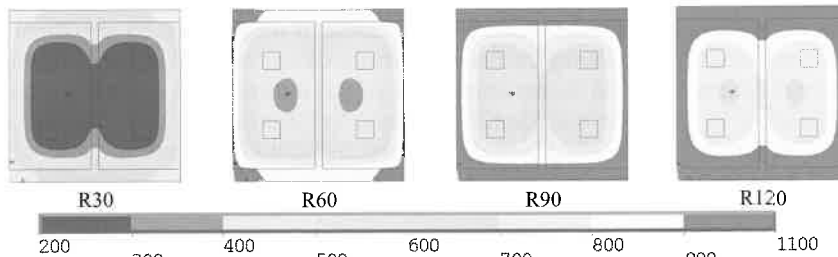


Fig. 3: Numerical results for section HEB 200 and for different fire ratings classes

The advanced calculation method used the following criteria to define the effect of fire in each component: The temperature of the flange, $\theta_{f,t}$ was determined by the arithmetic average of nodal temperature. The reduction of the web height, $h_{w,fi}$ was determined according to the 400 °C isothermal [7]. The residual cross section of concrete depends on the extension of concrete to be neglected, $b_{c,fi}$, being determined according to the 500 °C isothermal limit [6], while the temperature effect on steel reinforcement was calculated by the arithmetic average temperature of this component, see Fig. 2.

4. Balanced summation method

The effect of fire was determined for each component in 24 different cross sections, two different lengths and three different buckling lengths, giving a total of 144 axial buckling loads. The numerical results were compared to the existing formulas of Eurocode [1] and also to the new formulae [8].

4.1 Flange component

Fig. 4 represents the average temperature of the flange, depending on the section factor and on the standard fire resistance class. Each graph depicts the results of the simplified calculation method [1], the results of the advanced calculation method (ANSYS) and the results of the new formulae [8]. Eurocode 4 Part 1.2 presents conservative values for some sections factors and unsafe values to others. The average temperature of the flange of HEB and IPE sections is safe for standard fire R30, partially safe for R60 and unsafe for the remaining classes.

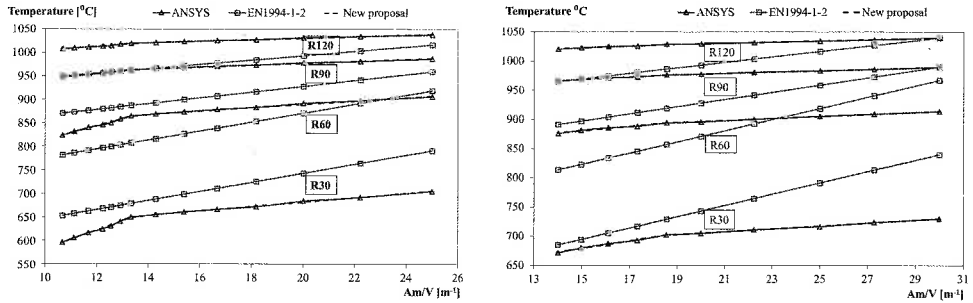


Fig. 4: Average temperature of the flange. HEB sections (left). IPE Sections (right)

The new proposal is based on the same formulae of Eurocode 4 Part 1.2 [1], Eq. 8, but using a bilinear approximation for temperature, using a new empirical coefficient k_t and a new reference value $\theta_{0,t}$, see Table 3.

$$\theta_{f,t} = \theta_{0,t} + k_t \left(A_m / V \right) \tag{8}$$

Table 3: Parameters to determine flange temperature (Section HEB and IPE)

Sections	$10 < A_m / V < 14$		$14 \leq A_m / V < 25$		$10 < A_m / V < 19$		$19 \leq A_m / V < 30$	
Standard	HEB		HEB		IPE		IPE	
Fire	$\theta_{0,t}$ [°C]	k_t [m°C]	$\theta_{0,t}$ [°C]	k_t [m°C]	$\theta_{0,t}$ [°C]	k_t [m°C]	$\theta_{0,t}$ [°C]	k_t [m°C]
R30	387	19,55	588	4,69	582	6,45	656	2,45
R60	665	14,93	819	3,54	824	3,75	862	1,72
R90	887	5,67	936	2,04	935	2,20	956	1,09
R120	961	4,29	998	1,62	997	1,68	1010	0,96

4.2 Web component

The effect of fire on the web of the cross section was determined by the 400 °C isothermal criterion. This procedure defines the affected zone of the web and predicts the web height reduction, see Fig. 5. The numerical results demonstrate a strong dependence on the section factor, regardless of the fire resistance class (t in minutes), unlike the simplified method of EN1994-1-2 [1]. The results of EN1994-1-2 [1] are unsafe for all fire resistance classes and for all section factors. The new proposal presents a parametric expression that depends on section factor and standard fire resistance class, Eqs. 9-10. Both equations have the application limits defined in Table 4.

$$2h_{w,f} / h_i \times 100 = 0.0035 \times t^2 \times (A_m / V) - 0.03 \times t^{2.02} + (A_m / V) / 2 \quad , (HEB) \tag{9}$$

$$2h_{w,f} / h_i \times 100 = 0.002 \times t^2 \times (A_m / V) - 0.03 \times t^{1.933} + (A_m / V) \quad , (IPE) \tag{10}$$

Table 4: Application limits for HEB and IPE cross sections

Standard fire resistance class	Section factor (HEB)	Section factor (IPE)
R30	$A_m/V < 22.22$	$A_m/V < 30.00$
R60	$A_m/V < 15.38$	$A_m/V < 18.56$
R90	$A_m/V < 12.22$	$A_m/V < 14.97$
R120	$A_m/V < 11.11$	-

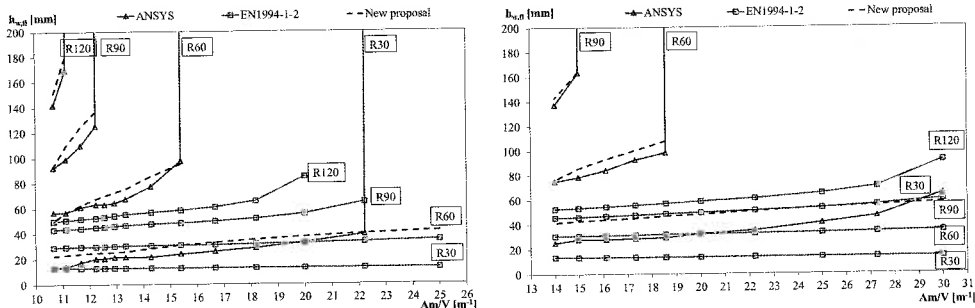


Fig. 5: Web height reduction. HEB sections (left). IPE Sections (right)

The arithmetic average temperature $\theta_{w,t}$ of the effective web section is depicted in Fig. 6 and was defined by the nodal position under the limiting condition, see Eq. 11 and Table 5. Temperature results of EN1994-1-2 were determined by the inverse method, using the reduction factor of the yielding stress $\sqrt{1 - 0.16(H_i/h)}$. The new proposal was adjusted to numerical results.

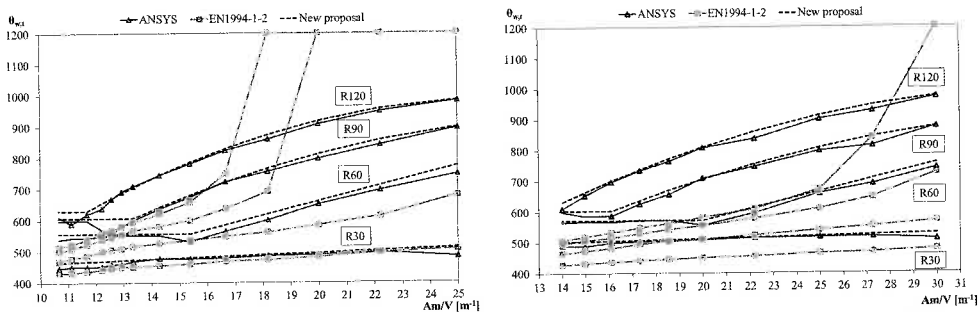


Fig. 6: Average web temperature for different standard fire resistance classes and sections. HEB sections (left). IPE Sections (right)

$$\theta_{w,t} = a \times (A_m/V)^2 + b \times (A_m/V) + c, \text{ (HEB, IPE)} \quad (11)$$

Table 5: Parameters and application limits for HEB and IPE cross sections

Standard fire resistance class	Section factor (HEB)			Section factor (IPE)				
	a	b	c	a	b	c		
R30	0.0000	3.2285	430.0000	10 < A_m/V < 25	0.0000	1.5708	480.0000	14 < A_m/V < 30
R60	0.0000	0.0000	566.6500	10 < A_m/V < 15	0.0000	0.0000	571.5400	14 < A_m/V < 20
	0.0000	22.5320	210.0000	15 < A_m/V < 25	0.0000	18.5770	200.0000	20 < A_m/V < 30
R90	0.0000	0.0000	606.4000	10 < A_m/V < 13	0.0000	0.0000	602.8100	14 < A_m/V < 15
	-1.1823	70.2440	-120.0000	13 < A_m/V < 25	-0.6761	50.7910	-40.0000	15 < A_m/V < 30
R120	0.0000	0.0000	629.8661	10 < A_m/V < 11	0.8283	57.6550	-15.0000	14 < A_m/V < 30
	-1.6136	85.6710	-150.0000	11 < A_m/V < 25	0.0000	1.5708	480.0000	14 < A_m/V < 30

4.3 Concrete component

The numerical result of the third component was determined by the 500 °C isothermal. The external layer of concrete to be neglected was measured in both principal directions, defining $b_{c,fi,vertical}$ and $b_{c,fi,horizontal}$. According to EN1994-1-2 [1], the thickness of concrete to be neglected depends on section factor, for standard fire resistance classes of R90 and R120. The numerical results demonstrates a strong dependence on section factors for all standard fire resistance classes.

Fig. 7 presents the new proposal for $b_{c,fi,vertical}$ and $b_{c,fi,horizontal}$ for HEB and IPE sections. Tables 6-7 provide the new formulae to determine the thickness of concrete to be neglected in fire design, based on the new Eq. 12, which applies to both cross section types (HEB and IPE) and directions (horizontal and vertical).

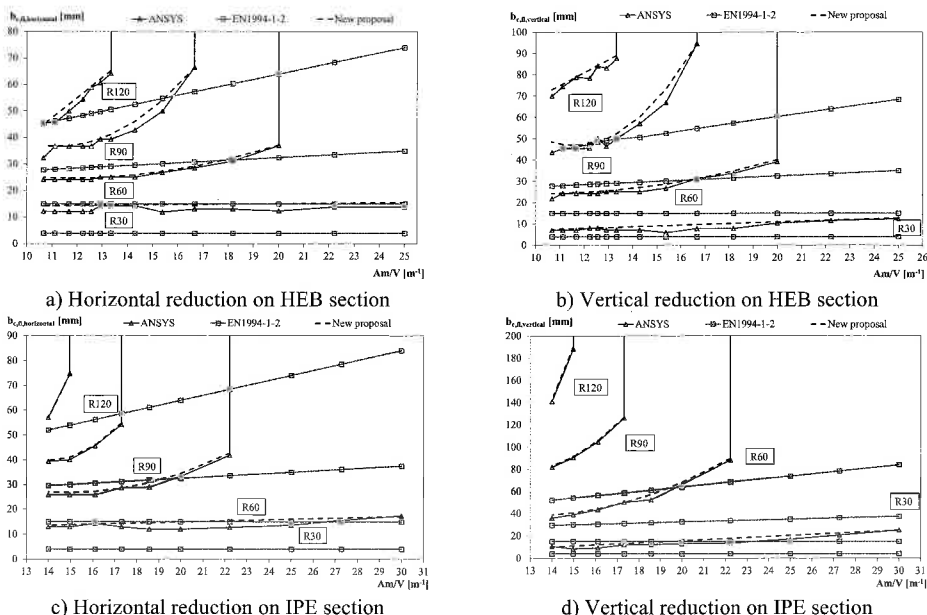


Fig. 7: Thickness reduction of the concrete area for HEB and IPE sections

$$b_{c,fi} = a \times (A_m/V)^2 + b \times (A_m/V) + c \tag{12}$$

Table 6: Parameters and application limits for thickness reduction of the concrete in sections HEB

Standard fire resistance class	$b_{c,fi,horizontal}$			$b_{c,fi,vertical}$			Section factor
	a	b	c	a	b	c	
R30	0,0000	0,0809	13,5	0,000	0,372	3,5	$10 \leq A_m/V \leq 25$
R60	0,1825	-4,2903	50,0	0,1624	-3,2923	41,0	$10 \leq A_m/V \leq 20$
R90	1,0052	-22,575	163,5	1,8649	-43,287	298,0	$10 \leq A_m/V \leq 17$
R120	0,0000	7,5529	-35,5	0,000	6,0049	9,0	$10 \leq A_m/V \leq 13$

Table 7: Parameters and application limits for thickness reduction of the concrete in sections IPE

Standard fire resistance class	$b_{c,fi,horizontal}$			$b_{c,fi,vertical}$			Section factor
	a	b	c	a	b	c	
R30	0,0000	0,2206	10,5	0,0000	0,9383	-3,0	$14 \leq A_m/V \leq 30$
R60	0,2984	-8,8924	93,0	0,5888	-15,116	135,0	$14 \leq A_m/V \leq 22$
R90	1,3897	-38,972	313,0	2,0403	-50,693	393,0	$14 \leq A_m/V \leq 17$
R120	0,0000	18,283	-199,0	0,0000	48,59	-537,0	$14 \leq A_m/V \leq 15$

The average temperature of the residual concrete section is represented in Fig. 8. The new proposal introduces a parametric approximation, based on the standard fire resistance and section factor, Eqs. 13-14. The application limits are presented in Table 8.

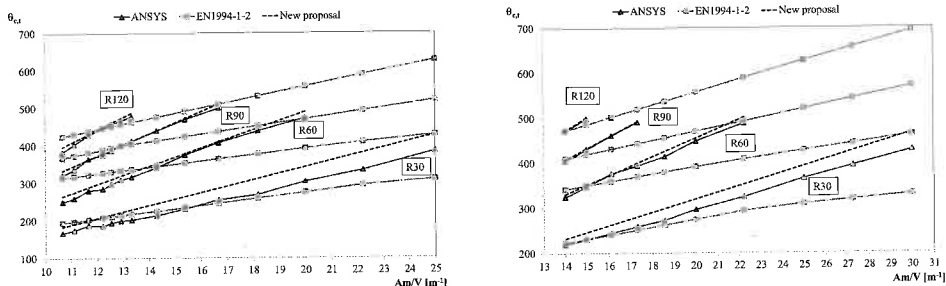


Fig. 8: Average temperature of residual concrete. HEB sections (left). IPE Sections (right)

$$\theta_{c,t} = +3.1 \times t^{0.5} \times (A_m/V) + 0.003 \times t^{1.95} \quad ,(HEB) \tag{13}$$

$$\theta_{c,t} = +2.67 \times t^{0.5} \times (A_m/V) + 3.4 \times t^{0.61} \quad ,(IPE) \tag{14}$$

Table 8: Application limits for average temperature of the concrete

Standard fire resistance class	Section factor (HEB)	Section factor (IPE)
R30	$A_m/V < 25$	$A_m/V < 30$
R60	$A_m/V < 20$	$A_m/V < 23$
R90	$A_m/V < 17$	$A_m/V < 18$
R120	$A_m/V < 14$	$A_m/V < 15$

4.4 Reinforcement component

Fig. 9 depicts the average temperature of rebars determined by the numerical results. The results of EN1994-1-2 [1] were indirectly determined through the most critical reduction factor. Alternatively, the new parametric formula is presented for the calculation of the average temperature of rebars. Eqs. 15-16 were developed to the new proposal, based on the distance between rebars exposed surface (u), fire resistance classe (t) and section facto (A_m/V).

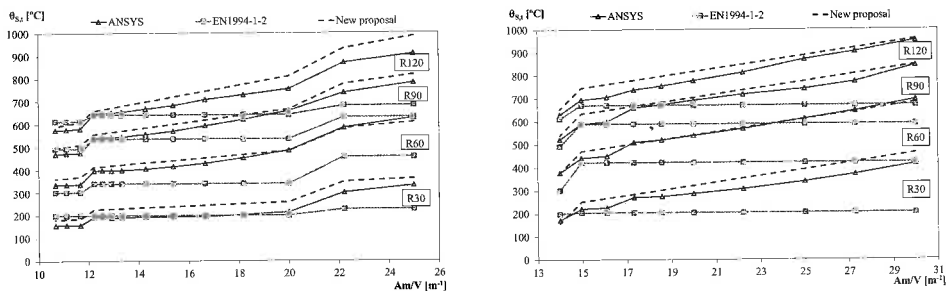


Fig. 9: Average temperature of rebars. HEB sections (left). IPE Sections (right)

$$\theta_{s,t} = 0.1 \times t^{1.1} \times (A_m/V) + 7.5 \times t - 0.1 \times t^{1.765} - 8 \times u + 390 \quad ,(HEB) \tag{15}$$

$$\theta_{s,t} = 14.0 \times (A_m/V) + 11.0 \times t - 0.1 \times t^{1.795} - 8 \times u + 115 \quad ,(IPE) \tag{16}$$

5. Axial buckling load under fire

The plastic resistance to axial compression and the effective flexural stiffness around the weak axis was calculated for 24 different cross section and four fire resistance classes. The ratio between both and the respective values at room temperature are represented in Fig. 10. The new formulae gives always safer and usually smaller results when compared to the existing formulae of Eurocode.

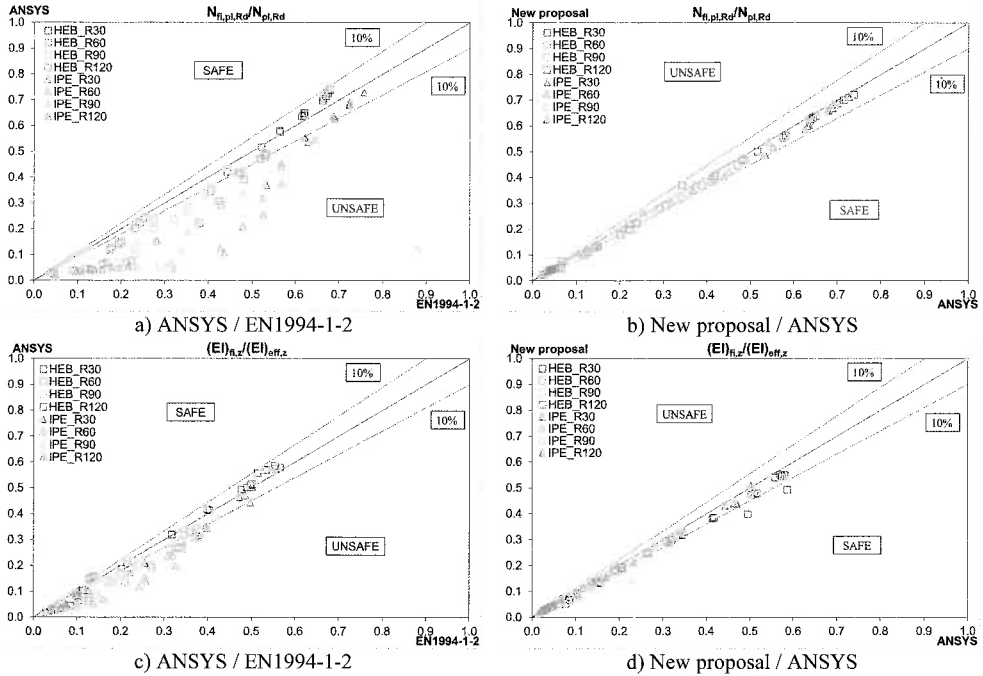


Fig. 10: Comparison of the dimensionless results

The elastic critical load will be smaller when calculated with the new formulae and the non-dimensional slenderness ratio under fire will be almost equal when calculated by both methods (Eurocode and new proposal). This fact produces design axial buckling loads, see Fig. 11.

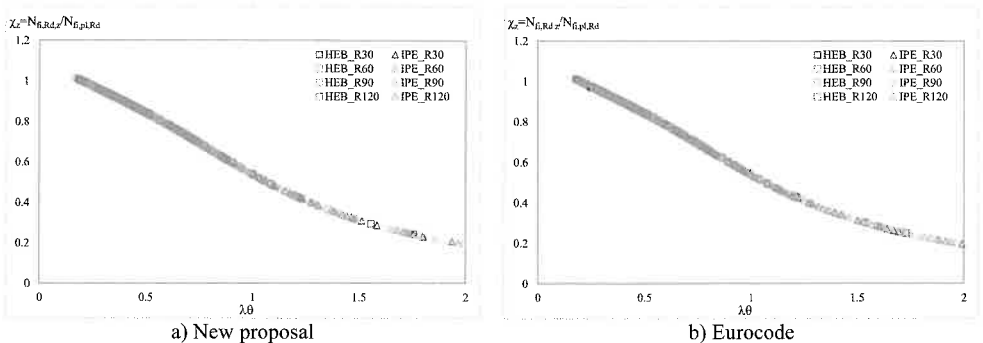


Fig. 11: Comparison of the reduction coefficient for axial buckling load, for both methods

6. Conclusions

24 simulations were developed to assess the fire behaviour of partially encased columns, in particular the new proposals to annex G of EN1994-1-2 [1]. This numerical simulations were developed by finite plane elements, and are only valid to standard fire exposure, running with ISO834 [2]. The simplified method proposed in Annex EN1994-1-2 G is unsafe for certain classes of fire resistance when compared to numerical results. This paper presented new formulae, with safety guarantee to the calculation of plastic resistance to axial compression and effective flexural stiffness of the cross-section with respect to the weak axis, under fire conditions. The design axial buckling load was compared for two different column lengths and for three different buckling lengths under fire.

References

- [1] CEN - EN 1994-1-2; *Eurocode 4 - Design of composite steel and concrete structures- Part 1-2: General rules - Structural fire design*; Brussels, August 2005.
- [2] ISO - ISO 834-1. *Fire-resistance tests - Elements of building construction – Part 1: general requirements*. Switzerland, Technical Committee ISO/TC 92: 25, 1999.
- [3] CEN, EN 1993-1-1 - *Eurocode 3: Design of steel structures - Part 1-1: General rules and rules for buildings*. Brussels. p. 91, 2005.
- [4] CEN, EN 1991-1-2 - *Eurocode 1: Actions on structures - Part 1-2: General actions - Actions on structures exposed to fire*, CEN: Brussels. p. 59, 2002.
- [5] CEN, EN 1993-1-2 - *Eurocode 3: Design of steel structures - Part 1-2: General rules - Structural fire design*, CEN: Brussels. p. 72, 2005.
- [6] CEN, EN 1992-1-2 - *Eurocode 2: Design of concrete structures - Part 1-2: General rules - Structural fire design*, CEN: Brussels. p. 97, 2004.
- [7] Cajot Louis-Guy (2012), Gallois Louis, Debruyckere Rik, Franssen Jean-Marc, Simplified design method for slim floor beams exposed to fire, *Proceedings of the Nordic Steel Construction Conference*, Oslo, Norway, 5-7 September, 2012.
- [8] Paulo Piloto, David Almeida, A. B Ramos-Gavilán, Luís M. R. Mesquita; “Partially Encased Section: Strength and Stiffness Under Fire Conditions”; pp: 15-18, *Book of Abstracts of the IFireSS – International Fire Safety Symposium*, ISBN 978-989-98435-3-0, pp: 29-38, Book of full papers ISBN 978-989-98435-5-4, ISSN 2412-2629, University of Coimbra, Portugal, 20th-22nd April 2015